Journal of Biomedical Optics

SPIEDigitalLibrary.org/jbo

Role of contrast and fractality of laser speckle image in assessing flow velocity and scatterer concentration in phantom body fluids

Cerine Lal
Arnab Banerjee
Narayanan Unni Sujatha

SPIE

Role of contrast and fractality of laser speckle image in assessing flow velocity and scatterer concentration in phantom body fluids

Cerine Lal, Arnab Banerjee, and Narayanan Unni Sujatha
Indian Institute of Technology Madras, Department of Applied Mechanics, Biophotonics Lab, Chennai 600036, India

Abstract. Blood flow velocity and red blood cell concentration are of vital importance in assessing tissue microcirculation. Laser speckle contrast analysis is being considered as a promising tool in the qualitative assessment of flow velocity as well as scatterer concentration in different body fluids, though the quantification part still remains challenging. The fractal-based spatial correlation analysis of speckle flow images along with the corresponding contrast analysis for the quantitative assessment of flow and scatterer concentration is investigated. In this study, phantom body fluid solution (intralipid 20%) of different concentrations is pumped at different flow rates through the designed flow channel using a syringe pump and the corresponding speckle images are acquired. The fractality of the acquired speckle images in response to the changes in concentration of the fluid as well as the variations in fluid flow is analyzed along with the corresponding contrast-based analysis. Following this qualitative analysis, an experimental model is attempted toward quantification of these parameters from a single acquired speckle image by considering the contrast and fractality changes together. [DOI: 10.1117/1.JBO.18.11.111419]

Keywords: laser speckle; contrast; scatterer concentration; flow velocity; fractality.

Paper 130280SSPRR received Apr. 26, 2013; revised manuscript received Oct. 17, 2013; accepted for publication Oct. 18, 2013; published online Nov. 18, 2013.

1 Introduction

Blood supplies nutrients and oxygen to all the parts of our body and also plays a major role in thermal regulation. Monitoring blood flow is, therefore, important and helps clinicians assess tissue health. Various diseases like diabetes, peripheral vascular disease, and Raynaud's phenomenon impair the tissue blood supply and, therefore, measurement of the same can provide information for the diagnosis/assessment of similar diseases. Changes in microvascular perfusion (tissue blood flow) are found to occur at the onset of a disease and hence, these changes, if detected, can provide early disease diagnosis, which in turn can increase the survival rates.

Laser speckle contrast imaging (LSCI) introduced in 1970s is a nonscanning, noninvasive wide field optical technique, which is being explored widely in microvascular perfusion assessment.[1] The principle of LSCI can be found elsewhere.[2,3] This technique was a breakthrough in the field of noninvasive monitoring of blood flow. Since then, various researchers have demonstrated a qualitative relationship between motion of scatterers and the resulting spatial or temporal speckle contrast of the integrated speckle pattern. LSCI offers good spatial and temporal resolution and has found applications in real-time blood flow imaging of retina and skin,[4–8] cerebral blood flow imaging,[9,10] monitoring of blood flow dynamics during neurosurgeries,[11] and also in photodynamic therapy.[12] Most of the discussed techniques rely on the variations in the contrast of the obtained speckle image.[5,13–15] Although LSCI has found tremendous applications in biomedical imaging, the quantification of flow velocities in its absolute units still remains a challenge and continues to be of increased research interest.[16–19] Although flow quantification has been tried out previously using alternate methods,[1,20–29] LSCI, due to its inherent advantage of whole field nature and noninvasiveness, holds a potential to be probed in quantitative studies.

It is imperative to keep the scatterer concentration uniform to ensure the relationship between speckle contrast and flow velocities while employing LSCI. As speckle image contrast is also dependent on the concentration of scattering centers, it is also possible to extract concentration related information by analyzing the contrast changes.[30] Hence, simultaneous variations of flow and scatterer concentration will be of great challenge to get assessed using LSCI. Extracting additional features of speckle pattern may enable the simultaneous extraction of flow and concentration details. Spatial and temporal speckle statistics, such as autocorrelation and power spectrum, have also been widely used to find the velocity and concentration of the moving scatterers, in addition to the texture analysis of surfaces and images.[31–34] Recently, fractal nature of the speckle patterns has also been proposed for characterization of rough surfaces, texture analysis, and spatial characterization of multiscattering medium.[35–37] The fractal analysis of LSCI data has also been carried out.[38] Our group has worked previously on the comparison of fractality of laser Doppler flow meter signals and laser speckle images acquired from different parts of the body in healthy subjects previously and has shown that the fractality of speckle images are found to be in agreement with the fractality Doppler signals in characterizing the flow changes.[39] From all these reported literature, the fractal nature of speckle

Address all correspondence to: Narayanan Unni Sujatha, Indian Institute of Technology Madras, Department of Applied Mechanics, Biophotonics Lab, Chennai 600036, India. Tel: +91 (0)44 2257 4067; Fax: +91 (0)44 2257 4052; E-mail: nsujatha@iitm.ac.in

0091-3286/2013/$25.00

pattern could be understood as an alternate tool in assessing flow or scatterer concentration–related parameters. In the present work, an experimental model is attempted analyzing the contrast and fractality features of a captured speckle pattern for extracting the flow velocity as well as scatterer concentration. The initially obtained results are found to be in agreement, suggesting the possible exploration for a more detailed and reliable quantified approach toward the synchronous analysis of multiple parameters related to fluid flow.

2 Materials and Methods

2.1 *Laser Speckle Imaging Experimental Setup*

The schematic of the experimental setup used in this study is shown in Fig. 1. Intralipid 20% solution (Fresenius Kabi, Bad Homburg, Germany) mimicking the body fluid of different concentrations (1%, 2%, 3%, 4%, and 5% v/v) is prepared and pumped at different flow rates through a phantom flow channel ranging from 10 to 190 ml/h in steps of 20 ml/h using a syringe pump (Model RH-SY10, Ravel Hiteks Pvt. Ltd, India).

The flow phantom was custom made by grooving channels of 3-mm width and 5-mm depth in perspex sheet (120×40 mm^2). The flow phantom was illuminated by diode pumped solid state laser (671 nm, 30-mW power) and speckle images were captured by the CCD camera (DCU223M, Thorlabs, Newton, NJ) zoom lens system. In the red and near-infrared region of light, most of the interactions in the tissue are scattering events rather than absorption events[40–42] and hence the choice of intralipid solution mainly representing the scatterers was made for the experiments. The distance between the CCD camera and the flow channel was maintained constant (40 cm) for all experiments. The laser source to sample distance was 15 cm. The optical setup provided a magnification of 1:1 and f number of 2.5, thus producing speckles of ~8.12 μm in diameter, which is approximately twice the pixel size of 4.65 μm, hence being optimal for speckle contrast imaging.[8]

Exposure time of the CCD camera was set to 20 ms, and subsequent image processing was done using MATLAB (Mathworks, Massachusetts).

2.2 *Laser Speckle Imaging of the Flow Channel—Contrast Analysis*

The acquired speckle image for the flow of intralipid 1% solution at a rate of 190 ml/h is shown in Fig. 2(a). For the spatial contrast analysis, the flow channel of size 500×21 pixels was selected and processed. The speckle contrast was calculated using Eq. (1) by taking 5×5 blocks of pixels over the entire channel image, thus producing a false color contrast map,[2] as shown in Fig. 2(b).

$$K = \frac{\sigma}{\langle I \rangle}, \tag{1}$$

where K is the speckle contrast, σ is the standard deviation, and $\langle I \rangle$ is the mean intensity. The average contrast of three maps corresponding to images taken with an interval of 10 s between them is calculated after enhancement procedures, which were adopted uniformly for different flow conditions.

2.3 *Laser Speckle Imaging of the Flow Channel: Fractal Analysis*

First order and second order statistics of speckle pattern have been used to analyze properties of the scattering media. First-order statistics describe the properties of speckle fields at each point. This includes intensity probability distribution function and contrast. Statistics of second order show how fast the intensity changes from point to point in the speckle pattern. Second-order statistics are described by autocorrelation function (g_2) of intensity fluctuations given by Eq. (2):[43]

$$g_2(x) = \langle I(x + \Delta x) I(x) \rangle, \tag{2}$$

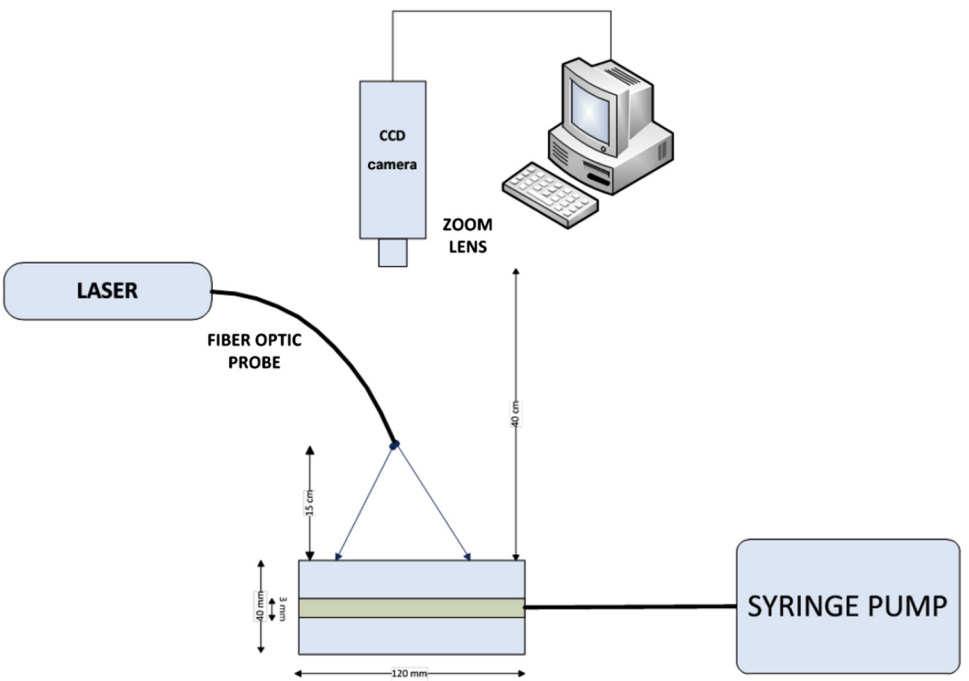

Fig. 1 Schematic of laser speckle imaging setup.

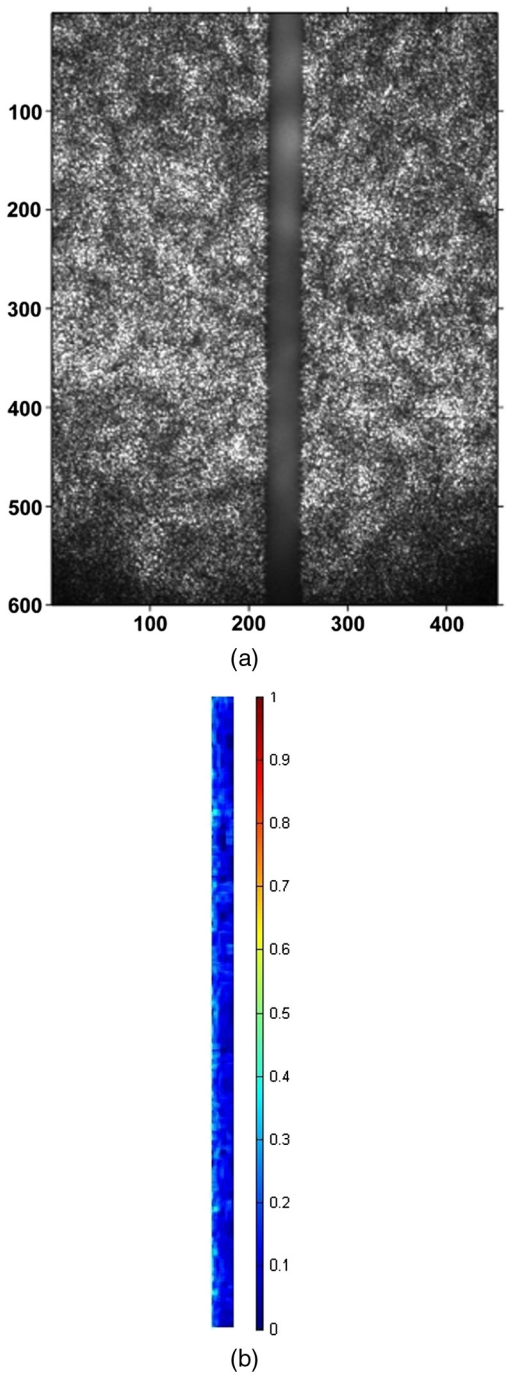

Fig. 2 (a) Raw speckle image and (b) speckle contrast image for 1% intralipid, 190 ml/h.

where x is the spatial or temporal variable, Δx denotes the change in the variable, and $I(x)$ is the intensity of speckle at x.

Small intensity fluctuations are described by autocorrelation function ($\tilde{g_2}$) of the form Eq. (3) and structure function (D) in Eq. (4) is used:[43]

$$\tilde{g_2}(\Delta x) = [\langle I(x+\Delta x) - \langle I \rangle \rangle][I(x) - \langle I \rangle] \tag{3}$$

$$D(\Delta x) = \langle [I(x+\Delta x) - I(x)]^2 \rangle. \tag{4}$$

The structure function is preferred over autocorrelation function while considering small scale intensity fluctuations. In the case of speckle image processing, structure function is preferred[37] and in the present work, we have analyzed the intensity fluctuations of the speckle pattern with variations in both flow and scatterer concentrations based on the structure function approach.

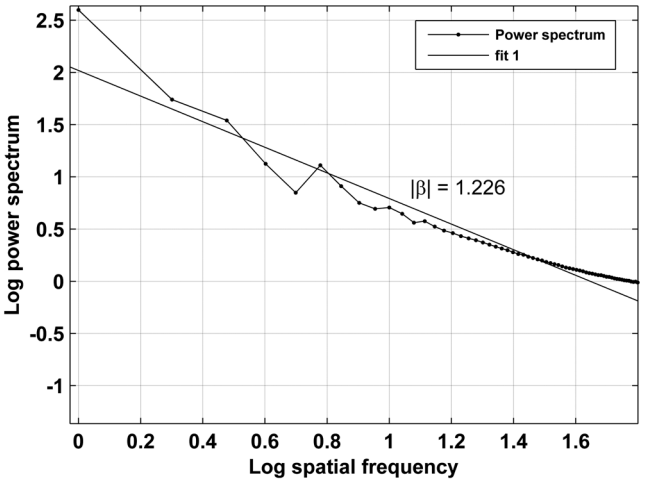

Fig. 3 Power law behavior of speckle intensity fluctuations ($|\beta| > 1$, hence the fractal Brownian motion).

The power law behavior of power spectral density of speckle intensity fluctuations characterizes self-similar processes, as shown in Fig. 3 and hence speckle statistics can be modeled by fractional Brownian motion as per the fractal theory,[35] and structure function of the speckle intensity fluctuations can be redefined by using a Brownian motion approach, wherein the variance of the process is proportional to the spatial or temporal increments as given by Eq. (5).

$$D(\Delta x) = \langle [I(x+\Delta x) - I(x)]^2 \rangle \propto \Delta x^{2H}, \tag{5}$$

where H is the Hurst coefficient ($0 < H < 1$).[35]

In our analysis, the structure function was calculated over each column of the channel image (500×21 pixels) considering the same images acquired as mentioned in Secs. 2.1 and 2.2 after subtracting the mean from the image, as given by Eqs. (6) and (7), and was averaged over all the columns.

$$I(x,y) = I(x',y') - \langle I(x',y') \rangle, \tag{6}$$

$$D(x, y+\Delta y) = \langle [I(x, y+\Delta y) - I(x,y)]^2 \rangle \propto \Delta y^{2H}, \tag{7}$$

where $I(x',y')$ represents the intensity at location (x',y') of the original image, $I(x,y)$ denotes the mean subtracted image, and $D(x, y+\Delta y)$ represents the variance of the intensity fluctuations along each column of the image.

The Hurst coefficient was calculated by fitting a regression line to the linear part of log–log plot of the increments in variance versus proximity of pixels in the image. The plot of the structure function versus pixel lag on a log–log scale is shown in Fig. 4 for intralipid concentrations of 1% and 5%, respectively, at flow rate of 190 ml/h.

H indicates the extent of correlation between successive elements of the signal.[44,45] $H > 0.5$ indicates that the stochastic process is positively correlated, i.e., an increasing trend in the past follows an increasing trend in the future and vice versa. $H <$ 0.5 indicates negative correlation or antipersistence indicating

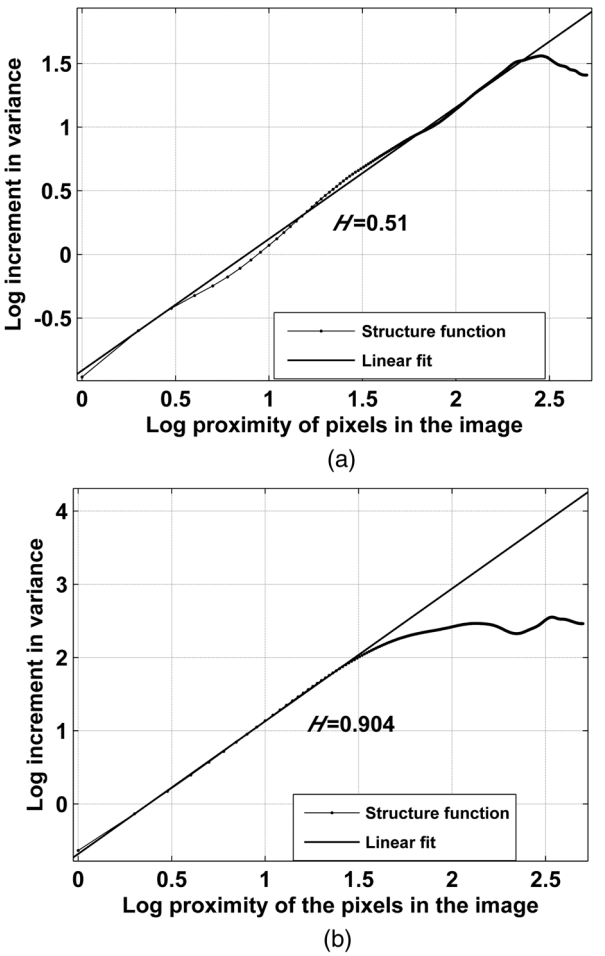

Fig. 4 Plot of the structure function with different concentrations of intralipid at flow rate 190 ml/h. (a) 1% intralipid and (b) 5% intralipid.

successive elements in the data following alternating increments and decrements.

3 Results and Discussions

The speckle images obtained for different flows and concentrations of intralipid solution, as mentioned in Sec. 2, were analyzed for the fractality and contrast. Table 1 shows the mean H and contrast values for different flow rates/flow velocities and intralipid concentrations along with the standard deviation measurements. The range of flow velocities is so chosen in order to represent the normal and varied range of tissue perfusion.[46]

3.1 *Variation of H with Flow Velocities*

An increasing trend was observed for H with an increase in the flow velocity. The fractional Brownian motion analyzed spatially in the intralipid fluid speckle image is found to be more positively correlated with increase in the flow velocity, as is evident from the increased H. The fractional Brownian motion, which could also be considered as a diffusion process exhibited in the speckle image spatial analysis, has previously been investigated for blood.[47] This could be seen as an effect to streamline or positively correlate the existing fractional Brownian motion with the effect of increased flow velocity. We hypothesize that the randomness in a fractional Brownian motion reduces with increased flow and this may be attributed to the cause of positive correlation seen with increased flow. An increase in H indicates that the variance of the intensity fluctuations as a function of the pixel location within the speckle images is increasing with increasing flow rates. A plot showing the relationship of H with flow velocity is shown in Fig. 5(a).

3.2 *Variation of H with Scatterer Concentration*

An increasing trend for spatial H is observed with increase in the concentration of the scatterers similar to that of the response for flow velocity. When the particle concentration is increased, the single particle chaotic movement may be restricted, facilitating particle agglomerations within the medium, which can be considered as the cause of increasing positive correlation for the fractional Brownian movement represented by the increased value of H corresponding to the spatial speckle image analysis. Also, as the scatterer concentration increases, the backscattered image intensity is increased as a result of more scattering centers in the medium leading to an increase in pixel intensity fluctuations, thereby increasing H. The relationship of H with scatterer concentration for constant flow velocities can be observed from Fig. 5(a).

3.3 *Variation of Speckle Contrast with Flow Velocity and Scatterer Concentration*

Analyzing average speckle contrast in the region of interest for flow analysis has been established by many researchers and is referenced widely in Sec. 1 of this article. As flow velocity increases, the image becomes blurred and the average contrast decreases. A plot showing the relationship of speckle contrast and flow velocity is shown in Fig. 5(b). It has also been established previously that the average speckle image contrast increases with increase in the scatterer concentration in static fluids[30] by our group. The dependence of speckle contrast on scatterer concentration and flow velocity can also be seen in reports.[48] We have observed a similar trend for different flows, with measurements being taken for a specific flow at a time. The relationship of scatterer concentration with speckle image contrast can be observed from Fig. 5(b).

3.4 *Dual Parametric Model for Simultaneous Scatterer Concentration and Flow Velocity Measurements*

From Figs. 5(a) and 5(b), it is observed that H and contrast follow an inverse relationship in the case of flow velocity. For a given concentration of intralipid and for increasing flow rates, H is increasing while the speckle contrast decreases. On the other hand, for a given flow velocity, increased H and contrast were observed with the increase in scatterer concentration. Also, it is observed that at higher scatterer concentrations, the change in H with varying flow velocities is less compared to that at lower concentrations.

As both Hurst coefficient and speckle contrast are found to be dependent on scatterer concentration and flow velocity, we have used multiple linear regression with our experimental data in order to model the dependence of scatterer concentration and flow rate on H and contrast. Below equations [Eqs. (8) and (9)] obtained represent the fitted plot, and corresponding plots are given along with the experimental results in Figs. 5(a) and 5(b). The parametric dependence (flow and scatterer concentration) of H as well as contrast was approximated to a linear fit

Table 1 Hurst coefficient (H) and speckle contrast (K) values for different velocities of flow (FLV) and scatterer (intralipid) concentrations in % V/V.

		Intralipid concentration									
	SC	1%		2%		3%		4%		5%	
Flow rate (ml/h)	FLV (mm/s)	H	K	H	K	H	K	H	K	H	K
10	0.185	0.252 ± 0.020	0.153 ± 0.0004	0.381 ± 0.004	0.148 ± 0.0005	0.470 ± 0.008	0.144 ± 0.0004	0.567 ± 0.007	0.140 ± 0.0002	0.8 ± 0.015	0.135 ± 0.0002
30	0.555	0.297 ± 0.013	0.150 ± 0.0009	0.470 ± 0.031	0.145 ± 0.0004	0.554 ± 0.013	0.142 ± 0.0001	0.653 ± 0.001	0.138 ± 0.0001	0.830 ± 0.013	0.135 ± 0.0003
50	0.925	0.310 ± 0.004	0.148 ± 0.0005	0.525 ± 0.004	0.143 ± 0.0006	0.564 ± 0.016	0.141 ± 0.0002	0.674 ± 0.001	0.135 ± 0.0001	0.834 ± 0.002	0.133 ± 0.0005
70	1.296	0.336 ± 0.007	0.146 ± 0.0001	0.533 ± 0.009	0.141 ± 0.0005	0.597 ± 0.007	0.139 ± 0.0002	0.688 ± 0.0005	0.133 ± 0.0002	0.839 ± 0.004	0.132 ± 0.0003
90	1.666	0.364 ± 0.007	0.145 ± 0.0005	0.561 ± 0.005	0.139 ± 0.0001	0.616 ± 0.008	0.136 ± 0.0008	0.693 ± 0.008	0.132 ± 0.0001	0.865 ± 0.004	0.130 ± 0.0004
110	2.073	0.384 ± 0.006	0.143 ± 0.0007	0.602 ± 0.002	0.138 ± 0.0003	0.642 ± 0.002	0.135 ± 0.0005	0.720 ± 0.002	0.130 ± 0.0002	0.872 ± 0.0013	0.127 ± 0.0002
130	2.407	0.394 ± 0.004	0.140 ± 0.0001	0.624 ± 0.01	0.136 ± 0.0003	0.653 ± 0.001	0.133 ± 0.0002	0.757 ± 0.003	0.128 ± 0.0001	0.873 ± 0.002	0.126 ± 0.0007
150	2.777	0.408 ± 0.005	0.138 ± 0.0006	0.651 ± 0.001	0.135 ± 0.0005	0.703 ± 0.007	0.131 ± 0.0001	0.816 ± 0.004	0.127 ± 0.0002	0.890 ± 0.002	0.124 ± 0.0007
170	3.148	0.441 ± 0.027	0.136 ± 0.0005	0.679 ± 0.009	0.133 ± 0.0002	0.831 ± 0.002	0.129 ± 0.0004	0.860 ± 0.008	0.125 ± 0.0006	0.891 ± 0.001	0.123 ± 0.0009
190	3.518	0.515 ± 0.013	0.135 ± 0.0003	0.710 ± 0.01	0.132 ± 0.0003	0.852 ± 0.0008	0.128 ± 0.0001	0.877 ± 0.001	0.124 ± 0.0001	0.904 ± 0.002	0.122 ± 0.0002

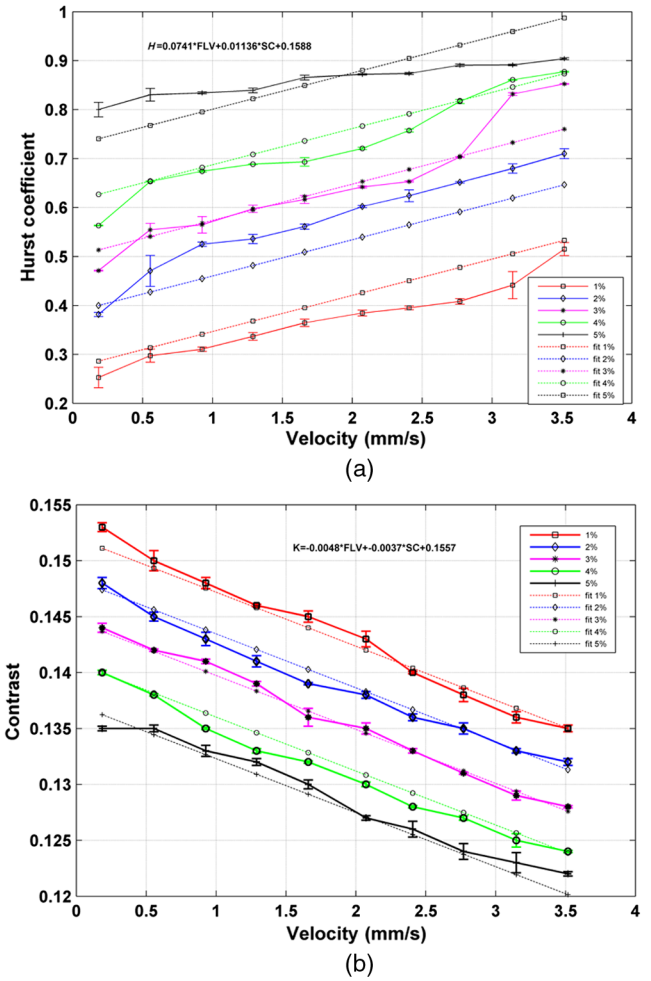

Fig. 5 (a) Plot of the experimental data and linear fit showing dependence of H on scatterer concentration and flow velocity. (b) Plot of the experimental data and linear fit showing dependence of contrast on scatterer concentration and flow velocity.

here, which can offer the possibility of assessing the parameters on a quantitative scale. This pilot study emphasizes that by taking a single-speckle pattern image of the region of interest and calculating its contrast as well as Hurst coefficient spatially can yield important information regarding the velocity of flow and concentration of scatterers present in the fluid.

$$H = 0.0741 * (\text{Flow velocity}) + 0.1136 * (\text{Scatterer concentration}) + 0.1588, \quad (8)$$

$$K = -0.0048 * (\text{Flow velocity}) - 0.0037 * (\text{Scatterer concentration}) + 0.1557. \quad (9)$$

4 Conclusion

The flow and scatterer concentration dependent variables of the speckle pattern image, such as contrast and Hurst coefficient, have been explored in this paper and could yield clear distinction between various flow values and scatterer concentrations. This is, in turn, intended to provide a quantitative assessment of flow velocities and scatterer concentrations, where the results provided an error within 5% limit. It is to be noted that the methodology discussed here yield a quantitative tool for assessing flow velocity and scatterer concentration simultaneously from a single acquired speckle pattern using simple instrumentation. The possible expression of these changes in a more analytical way will open up new directions in the field of LSCI. On the application side, this methodology can serve in the long run as a helping tool in characterizing normal and malignant tissues with associated variation in blood flow complexities and scatterer concentration based on the values of obtained Hurst coefficient as well as speckle contrast.

Acknowledgments

The authors acknowledge financial support from ICSR & IITM for carrying out the experimental research.

References

1. A. F. Fercher and J. D. Briers, "Flow visualization by means of single-exposure speckle photography," *Opt. Commun.* **37**(5), 326–330 (1981).
2. J. D. Briers and S. Webster, "Laser speckle contrast analysis (LASCA): a no scanning, full- field technique for monitoring capillary blood flow," *J. Biomed. Opt.* **1**(2), 174–179 (1996).
3. J. D. Briers, "Laser speckle contrast imaging for measuring blood flow," *Opt. Appl.* **37**(1–2), 139–151 (2007).
4. J. D. Briers, "Laser Doppler, speckle and related techniques for blood perfusion mapping and imaging," *Physiol. Meas.* **22**(4), R35–R66 (2001).
5. H. Y. Cheng et al., "Modified laser speckle imaging method with improved spatial resolution," *J. Biomed. Opt* **8**(3), 559–564 (2003).
6. H. Cheng and T. Q. Duong;, "Simplified laser-speckle-imaging analysis method and its application to retinal blood flow imaging," *Opt. Lett.* **32** (15), 2188–2190 (2007).
7. H. Cheng et al., "Laser speckle imaging of blood flow in microcirculation," *Phys. Med. Biol.* **49**(7), 1347–1357 (2004).
8. D. A. Boas and A. K. Dunn, "Laser speckle contrast imaging in biomedical optics," *J. Biomed. Opt.* **15**(1), 011109 (2010).
9. H. Y. Cheng et al., "Hyperosmotic chemical agent's effect on in vivo cerebral blood flow revealed by laser speckle," *Appl. Opt* **43**(31), 5772–5777 (2004).
10. S. Yuan et al., "Determination of optimal exposure time for imaging of blood flow changes with laser speckle contrast imaging," *Appl. Opt.* **44**(10), 1823–1830 (2005).
11. A. B. Parthasarathy et al., "Laser speckle contrast imaging of cerebral blood flow in humans during neurosurgery: a pilot clinical study," *J. Biomed. Opt.* **15**(6), 066030 (2010).
12. T. K. Smith et al., "Microvascular blood flow dynamics associated with photodynamic therapy and pulsed dye laser irradiation," *Lasers Surg. Med.* **38**(5), 532–539 (2006).
13. F. Domoki et al., "Evaluation of laser-speckle contrast image analysis techniques in the cortical microcirculation of piglets," *Microvasc. Res.* **83**(3), 11–317 (2012).
14. O. Yang and B. Choi, "Laser speckle imaging using a consumer-grade color camera," *Opt. Lett.* **37**(19), 3957–3959 (2012).
15. R. Liu, J. Qin, and R.K. Wang, "Motion-contrast laser speckle imaging of microcirculation within tissue beds in vivo," *J. Biomed. Opt.* **18**(6), 060508 (2013).
16. D. D. Duncan and S. J. Kirkpatrick, "Can laser speckle flowmetry be made a quantitative tool?," *J. Opt. Soc. Am. A Opt. Image Sci. Vis.* **25**(8), 2088–2094 (2008).
17. D. Briers et al., "Laser speckle contrast imaging: theoretical and practical limitations," *J. Biomed. Opt.* **18**(6), 066018 (2013).
18. B. Choi et al., "Linear response range characterization and in vivo application of laser speckle imaging of blood flow dynamics," *J. Biomed. Opt.* **11**(4), 041129 (2006).
19. A. K. Dunn, "Laser speckle contrast imaging of cerebral blood flow," *Ann. Biomed. Eng.* **40**(2), 367–377 (2012).
20. M. D. Stern, "*In vivo* evaluation of microcirculation by coherent light scattering," *Nature* **254**(5495), 56–58 (1975).
21. R. Bonner and R. Nossal, "Model for laser Doppler measurements of blood flow in tissue," *Appl. Opt.* **20**(12), 2097–2107 (1981).

22. A. Serov et al., "Laser Doppler perfusion imaging with a complimentary metal oxide semiconductor image sensor," *Opt. Lett.* **27**(5), 300–302 (2002).
23. M. N. Kim et al., "Noninvasive measurement of cerebral blood flow and blood oxygenation using near-infrared and diffuse correlation spectroscopies in critically brain-injured adults," *Neurocrit. Care* **12**(2), 173–180 (2010).
24. J. Hagblad et al., "A technique based on laser Doppler flowmetry and photoplethysmography for simultaneously monitoring blood flow at different tissue depths," *Med. Biol. Eng. Comput.* **48**(5), 415–422 (2010).
25. S. Margareta et al., "Non-invasive monitoring of muscle blood perfusion by photoplethysmography: evaluation of a new application," *Acta Physiol. Scand.* **183**(4), 335–343 (2005).
26. V. J. Srinivasan et al., "Optical coherence tomography for the quantitative study of cerebrovascular physiology," *J. Cereb. Blood Flow Metab.* **31**(6), 1339–1345 (2011).
27. J. D. Briers and S. Webster, "Laser speckle contrast analysis (LASCA): a no scanning, full- field technique for monitoring capillary blood flow," *J. Biomed. Opt.* **1**(2), 174–179 (1996).
28. D. Fixler and Z. Zalevsky, "Estimation of flow rate and direction of medium with low scattering coefficient via linear polarization measurement," *Opt. Lasers Eng.* **51**(2), 91–95 (2013).
29. D. Fixler et al., "Depolarization of light in biological tissues," *Opt. Lasers Eng.* **50**(6), 850–854 (2012).
30. A. K. Jayanthy, N. Sujatha, and M. Ramasubba Reddy, "Non-invasive assessment of static scatterer concentration in phantom body fluids using laser speckle contrast analysis technique," *Opt. Lasers Eng.* **49**(4), 553–556 (2011).
31. J. Churnside and H. Yura, "Velocity measurement using laser speckle statistics," *Appl. Opt.* **20**(2), 3539–3541 (1981).
32. N. Takai, T. Iwai, and T. Asakura, "Real-time velocity measurement for a diffuse object using zero-crossings of laser speckle," *J. Opt. Soc. Am.* **70**(4), 450–455 (1980).
33. A. Ohtsubo and J. A. Asakura, "Velocity measurement of a diffuse object by using time-varying speckles," *J. Opt. Quant. Electron.* **8**(6), 523–529 (1976).
34. A. Oulamara, G. Tribillon, and J. Duvernoy, "Biological activity measurement on botanical specimen surfaces using a temporal decorrelation effect of laser speckle," *J. Modern Opt.* **36**(2), 165–179 (1989).
35. S. Guyot, M. C. Péron, and E. Deléchelle, "Spatial speckle characterization by Brownian motion analysis," *Phys. Rev. E* **70**(4), 046618 (2004).
36. O. Carvalho et al., "Statistical speckle study to characterize scattering media: use of two complementary approaches," *Opt. Express* **15**(21), 13817–13831 (2007).
37. O. Carvalho, M. Benderitter, and L. Roy, "Noninvasive radiation burn diagnosis using speckle phenomenon with a fractal approach to processing," *J. Biomed. Opt.* **15**(2), 027013–027013 (2010).
38. A. H. Heurtier et al., "Laser speckle contrast imaging: multifractal analysis of data recorded in healthy subjects," *Med. Phys.* **39**(10), 5847–5849 (2012).
39. N. Sujatha and L. Cerine, "Laser based signal and image fractal analysis for assessment of blood flow," *Proc. SPIE* **8427**, 84272M (2012).
40. B. C. Wilson and S. L. Jacques, "Optical reflectance and transmittance of tissues: principles and applications," *IEEE J. Quantum Electron.* **26**(12), 2186–2199 (1990).
41. C. Simpson et al., "Near-infrared optical properties of ex vivo human skin and subcutaneous tissues measured using the Monte Carlo inversion technique," *Phys. Med. Biol.* **43**(9), 2465–2478 (1998).
42. R. Graaff et al., "Optical properties of human dermis in vitro and in vivo," *Appl. Opt.* **32**(4), 435–447 (1993).
43. V. V. Tuchin, *Tissue Optics: Light Scattering Methods and Instruments for Medical Diagnosis*, SPIE Press, Bellingham, WA (2007).
44. J. J. Collins and C. J. De Luca, "Open-loop and closed-loop control of posture: a random-walk analysis of center-of-pressure trajectories," *Exp. Brain Res.* **95**(2), 308–318 (1993).
45. A. Eke et al., "Physiological time series: distinguishing fractal noises from motions," *Eur. J. Physiol.* **439**(4), 403–415 (2000).
46. M. Stücker et al., "Capillary blood cell velocity in human skin capillaries located perpendicularly to the skin surface: measured by a new laser Doppler anemometer," *Microvasc. Res.* **52**(2), 188–192 (1996).
47. E. C. Eckstein, "Fractal Brownian motion and particle motions in blood flow," in *Annual Int. Conf. IEEE Engineering in Medicine and Biology Society*, Vol. 13, pp. 2240–2241, IEEE (1991).
48. A. B. Parthasarathy et al., "Laser speckle contrast imaging of flow in a microfluidic device," *Proc. SPIE* **6446**, 644604 (2007).